Dalton Transactions

ROYAL SOCIETY OF CHEMISTRY

PERSPECTIVE

View Article Online
View Journal | View Issue



Cite this: *Dalton Trans.*, 2023, **52**, 9525

# Recent trends in phenol synthesis by photocatalytic oxidation of benzene

Ziru Wang[a] and Einaga Hisahiro *[b]

Phenol is an important intermediate for manufacturing chemical products in industry. In recent decades, phenol synthesis by one-pot oxidation of benzene has aroused tremendous interest in phenol synthesis due to the enormous energy consumption of the three-step cumene method in the industry. Photocatalysis is promising for the selective conversion of benzene to phenol because it can proceed under mild reaction conditions. However, overoxidation of phenol by photocatalysts with high oxidation ability decreases the yield and selectivity, which is the major limiting factor. Thus, increasing the phenol formation efficiency plays a crucial role in photocatalytic systems for benzene oxidation. In this context, selective photocatalytic benzene oxidation over several types of photocatalytic systems has been developed rapidly in the past few years. In this perspective, current homogeneous and heterogeneous photocatalytic systems for this reaction have been reviewed systematically first. Then, an overview of some strategies from the last decade for increasing phenol selectivity has been provided. In the end, a summary and outlook on the challenges and future directions in the research field are included in this perspective, which would be of great interest for further improving the selectivity of the photocatalytic benzene oxidation reaction.

Received 8th May 2023,
Accepted 6th June 2023

DOI: 10.1039/d3dt01360j

rsc.li/dalton



## 1. Introduction

Synthetic organic chemistry is important in producing chemicals essential to human life, such as pharmaceuticals, agricultural chemicals, and food additives.[1] Among these chemicals, phenol (hydroxybenzene) is an important example since it is a precursor of the industrial production of many materials and useful compounds.[2–4] For example, phenol is a raw material for bisphenol A, which is important for producing polycarbonate. Another example is a phenolic resin produced from the reaction between phenol and substituted phenol with formaldehyde. Phenol can also be reduced to cyclohexanol, which is important for polyamide production. The annual production of phenol is 8.9 million tonnes worldwide, and most of them (~95%) are industrially produced from benzene by the three-step cumene process (Fig. 1a).[5] This process is energy-consuming due to the requirement of high temperature and high pressure. Moreover, the highly explosive cumene hydroperoxide is produced as an intermediate. In contrast, an equal amount of acetone as a byproduct was produced in the cumene process.[6]

One-pot oxidation of benzene to phenol has been actively studied as an alternative for phenol synthesis over the past few decades (Fig. 1b).[7–13] Most reported catalytic systems require harsh reaction conditions, such as high temperatures and pressures. Photocatalytic processes have attracted attention as "green" alternatives because they can activate benzene molecules using light as an energy source and convert them to phenol under mild reaction conditions.[14–16] Several photocatalysts have been developed for benzene oxidation to phenol by oxidants, including $H_2O_2$ and $O_2$.

Photocatalysis can be homogeneous and heterogeneous. Homogeneous photocatalysts such as organic photocatalysts and polyoxometalates (POMs) commonly show high activity for phenol formation but are difficult to be recovered after the reaction.[17–19] On the other hand, heterogeneous photocatalysts, mainly semiconductor-based photocatalysts, such as titanium dioxide ($TiO_2$), have been actively studied for the oxi-

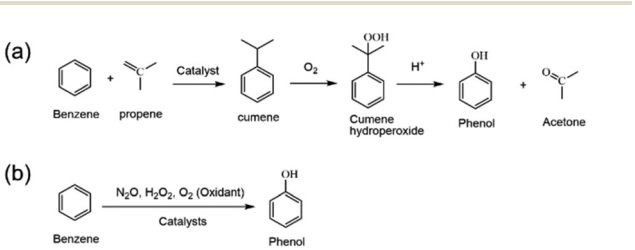


**Fig. 1** (a) Reaction steps for phenol synthesis *via* the cumene process; (b) one-pot oxidation of benzene to phenol.

[a]*Department of Molecular and Material Sciences, Interdisciplinary Graduate School of Engineering Sciences, Kyushu University, 6-1, Kasugakoen, Kasuga, Fukuoka 816-8580, Japan*
[b]*Department of Advanced Materials Science and Engineering, Faculty of Engineering Sciences, Kyushu University, 6-1, Kasugakoen, Kasuga, Fukuoka 816-8580, Japan. E-mail: einaga.hisahiro.399@m.kyushu-u.ac.jp*

dation of aromatic compounds.[20] Heterogeneous photocatalysts have the advantage that the catalyst and product are easily separated after the reaction. A major challenge in the photocatalytic oxidation of benzene to phenol is that phenol is easily overoxidized, and the selectivity of phenol is low. This is due to the formation of non-selective radicals and holes during the photocatalytic process. Furthermore, phenol is more reactive than benzene due to the lower bond energy of O–H in phenol (~371 kJ $mol^{-1}$) than the C–H bond energy in benzene (~473 kJ $mol^{-1}$).[21] Thus, various photocatalytic systems have been reported to increase phenol selectivity in benzene oxidation. Therefore, two aspects have been considered to suppress phenol overoxidation, including modification of photocatalysts and reaction conditions. Several review papers have reported one-pot oxidation of benzene to phenol in the past several years. Fukuzumi *et al.* reviewed the catalytic mechanism of the one-step selective hydroxylation of benzene to phenol.[22] Mancuso *et al.* summarized one-step catalysts or photocatalysts for oxidizing benzene to phenol in recent years.[14] Rahmani *et al.* summarized developments in transition metal-based mesoporous catalysts for the hydroxylation of benzene to phenol.[13] Han *et al.* reviewed heterogeneous photocatalytic hydroxylation of benzene to phenol since 2015.[23]

In this perspective, we comprehensively and historically summarize the design of homogeneous and heterogeneous photocatalysts to oxidize benzene to phenol using $H_2O_2$ or $O_2$ as an oxidant. Then, attention was turned to the most difficult and important issue in this research field: strategies to inhibit phenol overoxidation and increase phenol selectivity. Finally, the challenges of photocatalytic systems for producing phenol from benzene are noted, and future prospects are discussed.

## 2. Homogeneous photocatalysts

### 2.1 Organic homogeneous photocatalysts

Homogeneous photocatalysts have been extensively employed as efficient catalysts for one-pot benzene oxidation to phenol in the presence of oxidants such as $O_2$ and $H_2O_2$. The advantage of homogeneous systems is that the catalyst can be designed at the molecular level, and the active site structure can be homogeneous. As a result, homogeneous photocatalysts commonly showed high activity and high selectivity.

The first homogeneous photocatalyst for benzene oxidation to phenol was 3-cyano-1-methylquinolinium ion ($QuCN^+$) reported by Ohkubo *et al.* in 2011.[24] Due to the strong oxidizing ability at the singlet excited state ($E_{red}$ *vs.* the SCE = 2.72 V), $QuCN^+$ efficiently oxidized benzene to phenol (Fig. 2a). In addition, phenol was also generated when 1-methylquinolinium ($QuH^+$) and 1,2-dimethylquinolinium ($QuMe^+$) were utilized instead of $QuCN^+$. The reaction catalyzed by $QuCN^+$ was initiated by the electron transfer from benzene to UV light-excited $QuCN^+$ ($QuCN^{+}*$). In these quinoline ion-based systems, $O_2$ was selected as an easily available green oxidant. The benzene cation radical readily reacted with water

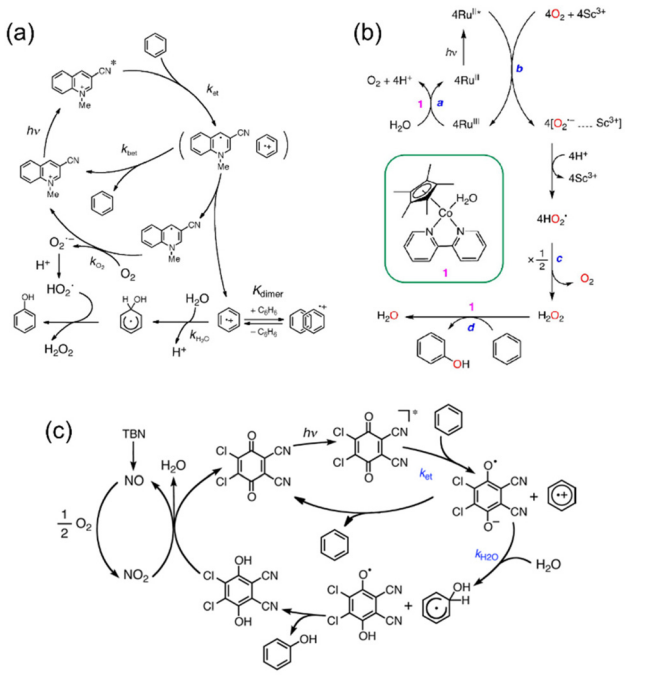


**Fig. 2** Reaction mechanisms for organic homogeneous photocatalysts. (a) QuCN+; adapted with permission from ref. 21. Copyright 2011 Wiley. (b) $[RuII(Me_2phen)_3]^{2+}$ with $[CoIII(Cp^*)(bpy)(H_2O)]^{2+}$; adapted with permission from ref. 28. Copyright 2017 RSC. (c) 2,3-Dichloro-5,6-dicyano-*p*-benzoquinone (DDQ), *tert*-butyl nitrite (TBN), and $N_2O$. Adapted with permission from ref. 29. Copyright 2013 ACS.

to give an □OH adduct radical, which then reacted with the $HO_2^{\bullet}$ radical derived from $O_2$ reduction to give $H_2O_2$. Thus, an equal amount of $H_2O_2$ is generated simultaneously with phenol in this system. The high activity of the quinoline ion as a homogeneous photocatalyst for benzene oxidation has been further reported by Long *et al.*[25] Their work proposed that a commercially available quinoline sulfate ($QuH_2SO_4$) acted as the photocatalyst, although the phenol yield was lower than that of $QuCN^+$. This result also indicates that the anion influences the photocatalytic activity of the quinoline cation. Zheng *et al.* developed a dual catalytic system in an anaerobic system without any oxidant, which coupled $QuCN^+$ and a cobalt catalyst in 2016.[26] In this system, phenol was produced from benzene and water by using the quinoline ion as the photocatalyst. In contrast, cobalt catalysts reoxidized the reduced quinoline ion and produced $H_2$ to complete the catalytic cycle. The above result indicates that the quinoline ion is an efficient homogeneous organic photocatalyst for benzene oxidation to phenol in the presence and absence of $O_2$ as the oxidant.

Compared with $O_2$, $H_2O_2$ is a more efficient oxidant for benzene oxidation to phenol because highly active radicals are easily formed. Asghari *et al.* introduced iron(II) phthalocyanine (FePc) as an efficient photocatalyst for benzene oxidation with $H_2O_2$ in acetonitrile as a solvent (2020).[27] The FePc catalyst was prepared by microwave irradiation during the cyclotetramerization of phthalic anhydride in the presence of iron(II) sulfate and urea. The *in situ* generated $H_2O_2$ can function as

 

an oxidant for benzene oxidation to phenol in an $O_2$-saturated solvent mixture of acetonitrile and $H_2O$ (v/v = 23 : 2) containing $Sc(NO_3)_3$.[28] In this system, $[RuII(Me_2phen)_3]^{2+}$ acted as a photocatalyst for efficient $H_2O_2$ production by $O_2$ activation in the presence of $Sc(NO_3)_3$. A cocatalyst ($[CoIII(Cp^*)(bpy)(H_2O)]^{2+}$) can efficiently utilize the generated $H_2O_2$ for subsequent benzene oxidation (Fig. 2b). Being environmentally benign, $H_2O_2$ and $O_2$ are the most frequently used oxidants in photocatalytic benzene oxidation. Another oxidant has been rarely reported unless the very high activity. For example, an efficient system was reported by Ohkubo *et al.* in 2013, in which light-excited 2,3-dichloro-5,6-dicyano-*p*-benzoquinone (DDQ) was utilized as a powerful oxidant for benzene oxidation by electron transfer in an $O_2$ saturated acetonitrile solution (Fig. 2c).[29] Then, *tert*-Butyl nitrite (TBN) can be used as a recycling reagent to convert $DDQH_2$ to DDQ *via* $NO_2$ under aerobic conditions.

Organic homogeneous photocatalytic systems commonly show highly efficient benzene oxidation to phenol. However, they are expensive or need additional cocatalysts and oxidants, increasing the operating cost.

### 2.2 Inorganic homogeneous photocatalysts

Polyoxometalates (POMs) and heteropolyacids (HPAs) are representative inorganic homogeneous photocatalysts that are relatively inexpensive, have high structural stability, and can oxidize benzene to phenol. They are anionic nanoclusters of early transition metal oxides that adopt various structures.[30–32] HPA with the Keggin structure has been most widely studied because of its thermal stability and high activity in various catalytic reactions.[33] As shown in Fig. 3, the Keggin structure has a central tetrahedron ($XO_4$, X = P, Si...) surrounded by four vertex-sharing trimers ($M_3O_{13}$, M = Mo, W, V...). Each trimer has three octahedral units ($MO_6$), which are linked in a triangular arrangement by sharing edges. They can be used as photocatalysts, as they absorb near-ultraviolet light and are excited to be highly reactive chemical species (HPA*).[34–36] The HPA* species acts as a better oxidant than HPA in the ground state for the oxidation of organic substrates, resulting in the formation of products and heteropolyblues (the reduced state of HPA). The generated heteropolyblue is then readily reoxidized by $O_2$ to complete the catalytic cycle.

In 2005, Park *et al.* first reported that Keggin-type HPA exhibited activity comparable to $TiO_2$ in photocatalytic benzene oxidation in an aqueous solution.[37] As in the case of $TiO_2$, phenol overoxidation over HPAs was inevitable, and the selectivity was low in this system. The oxidation of benzene to phenol with a vanadium tungsten polyoxometalate $NaH_3PW_{11}VO_{40}$ was then investigated in a dual-phase system by Schulz *et al.*[38] The authors found that benzene was very efficiently photo-oxidized to phenol under light irradiation. This process was accompanied by the reduction of the photocatalyst as indicated by a color change from yellow to violet-blue and the formation of a vanadium(IV) multiline EPR signature. These reduced photocatalysts were not reoxidized with $O_2$, which needed additional electron acceptors such as $Fe^{3+}$ and $HNO_3$. However, these electron acceptors dramatically decreased the phenol selectivity.

Recently, we have reported that POMs can be utilized as inorganic homogeneous photocatalysts using $O_2$ as an oxidant without adding other reagents under aerobic conditions.[21] For example, $H_3PW_{12}O_{40}$, a commercially available catalyst, showed a high phenol yield and selectivity in a 50% acetonitrile solution under ambient conditions (Fig. 4).[21] The excited state of $H_3PW_{12}O_{40}$ ($PW_{12}O_{40}^{3-*}$) can oxidize benzene to give a benzene cation radical, while $H_3PW_{12}O_{40}$ reduced to heteropoly blue. The kinetic isotope effect (KIE) showed that this process obeys the electron transfer (ET) process but not the hydrogen atom transfer (HAT) process. The benzene cation radical generated phenol in the presence of $H_3PW_{12}O_{40}$ and $H_2O$. Then, the reduced $H_3PW_{12}O_{40}$ was readily reoxidized with $O_2$ in air to give $H_2O_2$. The *in situ*-generated $H_2O_2$ can also be an oxidant to reoxidize the reduced $H_3PW_{12}O_{40}$ to generate a highly active OH radical for benzene oxidation to phenol by another minor route. Compared with the homogeneous organic systems, the advantages of this inorganic system are the low price of $H_3PW_{12}O_{40}$, requirement of no additional reagent, and high stability. In addition, this high stability of $H_3PW_{12}O_{40}$ ensures that it can be recovered after reaction with rotary evaporation for recycling of at least 5 cycles.

As another common polyoxometalate, decatungstate has been widely utilized for photocatalytic synthesis.[39] However, it

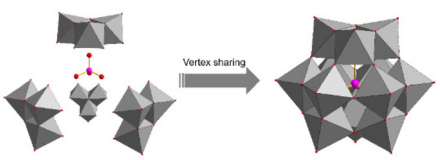


**Fig. 3** The structure of POMs with the Keggin structure.

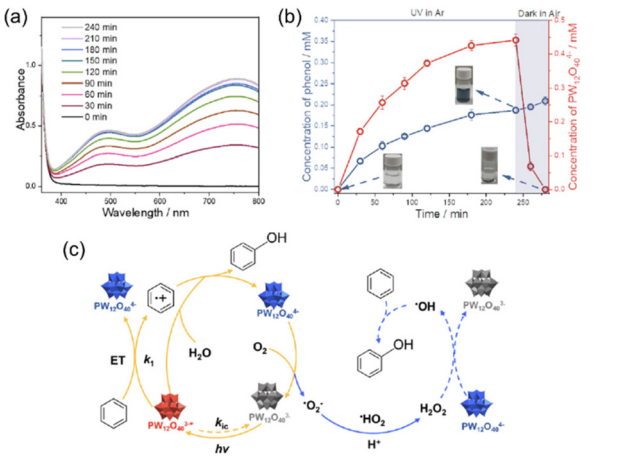


**Fig. 4** (a) UV-vis spectra of the reaction solution after 30, 60, 90, 120, 150, 180, 210, and 240 min of irradiation under argon; (b) time course for the phenol formation under anaerobic conditions; (c) proposed mechanism of the photocatalytic oxidation of benzene to phenol with $O_2$.

**Table 1** Catalytic performance of homogeneous photocatalysts for benzene oxidation to phenol

| Photocatalysts | Reaction conditions | Yield/% | Selectivity/% | Ref. |
|---|---|---|---|---|
| $QuCN^+$ | 500 W xenon lamp ($\lambda$ = 290–600 nm), 30 mM benzene, $O_2$, Acetonitrile, 1 h | 30 | 98 | 24 |
| $QuH_2SO_4$ | 500 W mercury lamp ($\lambda$ > 290 nm, 200 mM benzene, $O_2$, aqueous acetonitrile solution (80 vol%), 10 h | 11 | — | 25 |
| $QuCN^+/Co(dmgBF_2)_2(CH_3CN)_2$ | 300 W mercury lamp ($\lambda$ > 300 nm), 10 mM benzene, without oxidant, acetonitrile, 5 h | 90 | 100 | 26 |
| $[RuII(Me_2phen)_3]^{2+}/[CoIII(Cp^*)(bpy)(H_2O)]^{2+}$ | $\lambda$ > 420 nm, 1 mM benzene, $O_2$, mixture of acetonitrile and $H_2O$ (v/v = 23 : 2), 24 h | 30 | — | 28 |
| $NaH_3PW_{11}VO_{40}$ | 100 W mercury lamp ($\lambda$ > 200 nm), 1.58 mM benzene, $O_2$, acetonitrile, 5 h | 25 | 63 | 38 |
| $H_3PW_{12}O_{40}$ | 300 W xenon lamp ($\lambda$ > 300 nm), 30 mM benzene, $O_2$, mixture of acetonitrile and $H_2O$ (v/v = 1 : 1), 24 h | 41 | 80 | 21 |
| $Na_4W_{10}O_{32}$ | 300 W xenon lamp ($\lambda$ > 300 nm), 8.5 mM benzene, $O_2$, mixture of $H_2O$ and acetic acid (v/v = 5 : 1), 2 h | 31 | 74 | 39 |

can hardly activate C–H in the benzene molecule due to the high band activation energy *via* a HAT process in an organic solvent. Our group found that an efficient ET process occurred in an aqueous acetic acid solution. In this system, a reaction mechanism similar to that of $H_3PW_{12}O_{40}$, which is different from $TiO_2$, has been proposed. Notably, the phenol production in this decatungstate system was higher than that in other polyoxometalates and semiconductor-based photocatalysts.

The results of photocatalytic hydroxylation of benzene to phenol using homogeneous photocatalysts are summarized in Table 1. In homogeneous systems using molecular photocatalysts, the difficulty in recovering the photocatalyst after the reaction is a major limiting factor in its application.

Therefore, immobilizing the photocatalyst on supporting supported photocatalysts as heterogeneous catalysts for benzene oxidation has rarely been reported, although they have been reported for other selective oxidation reactions. A possible reason is that the oxidizing ability of the molecular photocatalyst is weakened by being immobilized on the supporting materials, which alters the reaction rate and reduces its activity. Another *n* is the leaching of active species from the supported photocatalysts during the reaction, especially in a solvent with high polarities, namely water.

## 3. Heterogeneous photocatalysts

Heterogeneous photocatalysts have advantages such as low cost and easy separation from reaction products. Studies have been conducted on benzene oxidation reactions using $TiO_2$, $C_3N_4$, $WO_3$, MOFs, and other photocatalysts. These catalysts have their specific characteristics based on their activities and selectivities.

### 3.1 Titanium dioxide ($TiO_2$)

Titanium dioxide ($TiO_2$) is the first and most reported photocatalyst for benzene oxidation after Honda and Fujishima found that it can simultaneously produce electrons and holes for subsequent reactions under UV light irradiation in 1972.[20] It showed high activity due to the suitable band structure and capability of active species generation. Until now, both $H_2O_2$ and $O_2$ have been utilized as the oxidants for benzene oxidation in the $TiO_2$ systems. $H_2O_2$ is an efficient oxidant for benzene oxidation due to the generation of highly active hydroxyl radicals ($^{\bullet}OH$).[40–42] The $^{\bullet}OH$ radical directly attacks benzene to produce phenol *via* a hydroxycyclohexadienyl radical as an important intermediate. However, raw $TiO_2$ showed low activity for benzene oxidation due to the fast recombination of electron–hole pairs and low efficiency for $H_2O_2$ activation. Thus, suitable decoration methods, including doping or heterojunction formation, are needed to improve the activity. For example, Fe and Cr dual-doped nanocrystalline titania ($Ti_{1-x-y}M_{x+y}O_2$) has been synthesized for highly selective photocatalytic conversion of benzene to phenol with $H_2O_2$ as the oxidant (2018).[43] $TiO_2$ doped with Fe ($Ti_{0.98}Fe_{0.02}O_2$) showed higher catalytic activity for benzene oxidation, indicating the importance of introducing Fe. Introducing Cr as a second doping atom ($Ti_{0.98}Fe_{0.01}Cr_{0.01}O_2$) further enhanced the phenol yield, which was ~2 times higher than that with $Ti_{0.98}Fe_{0.02}O_2$. The increased photocatalytic activity of $Ti_{1-x-y}M_{x+y}O_2$ was mainly due to the generation of an electron trapping level composed of $Fe^{3+}$ and $Cr^{3+}$ in the $TiO_2$ conduction band. As shown in Fig. 5, Fe doping improves electron–hole pairing separation, and Fe plays an important role in OH– formation and phenol formation through $H_2O_2$ activation (Path-A). The holes also react directly with benzene to form benzene cation radicals, giving phenol (Path-B). The same group reported $Cu(OH)_2$ decorated on two-dimensional (2D)

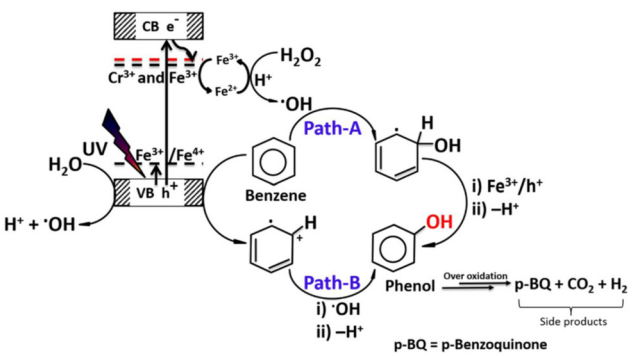


**Fig. 5** Possible mechanism of photocatalytic benzene oxidation to phenol by Fe and Cr dual-doped nanocrystalline titania ($Ti_{1-x-y}M_{x+y}O_2$). Adapted with permission from ref. 43 Copyright 2018 ACS.

 

dual-phase mesoporous leaf titania (LT) for photocatalytic benzene oxidation to phenol by $H_2O_2$. The $Cu(OH)_2$ modification improves electron–hole pair separation and activates $H_2O_2$ for benzene oxidation, a role similar to that of $Fe^{3+}$ in $Ti_{0.98}Fe_{0.01}Cr_{0.01}O_2$.

Apart from a transition metal, noble metal decoration could also enhance the photocatalytic benzene oxidation to phenol. Hosseini *et al.* synthesized Au–Pd NPs on the surface of carbon fiber felt (CFF) coated with amorphous $TiO_2$ for enhanced photocatalytic benzene oxidation to phenol with $H_2O_2$ under mild conditions.[44] In another work, Pd nanoparticles and $CeO_2$ were decorated on $TiO_2$ ($Pd/CeO_2/TiO_2$).[45] The synergic effect between the active metal and supports was important for excellent catalytic activity.

Above $TiO_2$-based systems utilized $H_2O_2$ as an efficient oxidant for benzene oxidation, but its high price is a major limitation of its application. $O_2$ is an ideal oxidant, especially when available directly from air. $TiO_2$ has been extensively used as a photocatalyst for multiple oxidation reactions by $O_2$, especially in organic pollutant degradation. Bui *et al.* (2010) systematically studied the photocatalytic benzene oxidation process using isotopic oxygen tracers ($H_2{}^{18}O$ and $^{18}O_2$) in aqueous solutions with different $TiO_2$ powders.[46] In their work, the crystal phase of $TiO_2$ was found to play an important role in the activity and reaction pathway for benzene to phenol. The anatase powder showed higher activity than rutile powder. They proposed that benzene oxidation by $TiO_2$ can be considered to be due to either oxygen transfer or hole transfer. The former is likely *via* a complicated intermediate from water, including $^{\bullet}OH$, Ti–$O^{\bullet}$, Ti–$OO^{\bullet}$, or more complicated surface peroxides. The pathway has been well known as the main reaction pathway for benzene oxidation by $TiO_2$, as shown in Fig. 6. Their work revealed that phenol was also generated using $O_2$ as an oxygen source *via* the hole transfer pathway. The generated hole can directly oxidize benzene to a benzene cation radical as an important reaction intermediate that reacts with $O_2$ to form phenol. These holes can also oxidize water to give $^{\bullet}OH$, which can attack benzene to give phenol through a reductive process. On the other hand, $O_2$ can be activated and reduced to reactive oxygen species, which also contribute to phenol formation. In addition, $O_2^{\bullet-}$ generated from the reduction of $O_2$ can be used in the reaction with benzene cation radicals. The pathway using water as an oxygen source is important in the efficient oxidation of benzene, and is the major pathway of anatase powder. Conversely, $O_2$ is involved in phenol formation, and $O_2$ reduction is the main pathway of rutile powder.

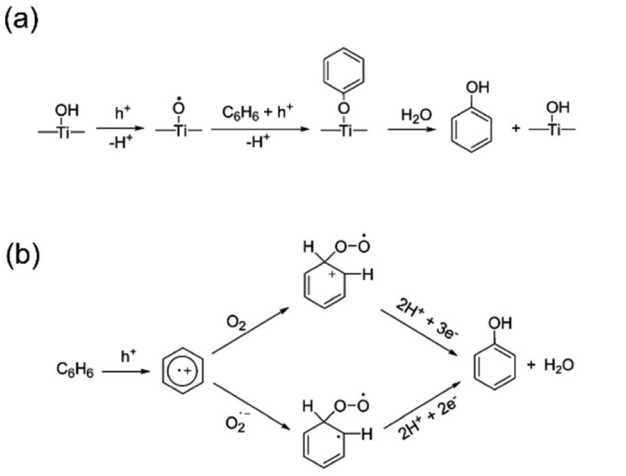


Fig. 6 Possible mechanism of photocatalytic benzene oxidation *via* oxygen transfer (a) and hole transfer (b). Adapted with permission from ref. 46. Copyright 2010 ACS.

Like the $TiO_2$-based systems utilizing $H_2O_2$, the doping and metal particle loading effectively increase the activity of $TiO_2$ by using $O_2$ as an oxidant. Devaraji *et al.* synthesized V-doped anatase $TiO_2$ ($TV_2$, $Ti_{0.98}V_{0.02}O_2$) by a solution combustion method and used it for photocatalytic benzene oxidation to phenol in a biphasic system under photoirradiation.[47] Charge carrier generation was promoted due to the formation of Schottky junctions of Au and $Ti_{0.98}V_{0.02}O_2$, which reduced the recombination of the excited electron–hole pair and increased the migration of electrons and holes for benzene oxidation. The hole was the main active species for benzene oxidation to phenol *via* the formation of a benzene cation radical. The Au particle does not seem to be the active species for benzene oxidation, although it absorbed visible light through surface plasmon resonance (SPR). Au and V acted as electron sinks to increase the electron–hole separation for benzene oxidation by holes.

In another study by Dasireddy *et al.*, a noble metal-free photocatalyst for benzene oxidation to phenol was prepared by loading copper and anatase $TiO_2$ on multi-walled carbon nanotubes (CNT).[48] The positively charged CNT can draw the electrons from the valence band of $TiO_2$, improving the following benzene oxidation reaction by the holes. Furthermore, the titanium–oxygen–carbon bonds (Ti–O–C) formed between $TiO_2$ and CNT enhanced the light absorption and photocatalytic activity.

### 3.2 Carbon nitride ($C_3N_4$)

Carbo nitride ($C_3N_4$) as a visible light-responsible photocatalyst has received wide attention due to its advantages, such as a moderate bandgap (2.7 eV), low cost, good stability, and easy preparation. Since the first report on photocatalytic $H_2$ evolution over $C_3N_4$ by Wang *et al.* in 2009, many efforts have been devoted to improving the performance of $C_3N_4$ under visible light ($\lambda > 420$ nm) for various reactions.[49–53]

The first example of photocatalytic benzene oxidation to phenol by $C_3N_4$ was reported by Chen *et al.* in 2009.[54] Fe-doped $C_3N_4$ exhibited enhanced activity for photocatalytic benzene oxidation to phenol by $H_2O_2$ under visible light. The leaching experiment of Fe indicates that phenol was formed mainly by the heterogeneous photocatalytic reaction. In addition, the loading of Fe-doped $C_3N_4$ on SBA-15 (Fe-g-$C_3N_4$/SBA-15) significantly improved the photocatalytic performance due to the increased surface area. The same group also reported that the supporting material was important for

phenol formation.[55] When they used titanium silicate zeolite (TS-1) instead of SBA-15, the phenol yield significantly increased due to the promoting effect of $H_2O_2$ activation by TS-1.

Besides Fe doping, combining $FeCl_3$ with $C_3N_4$ improved the activity for photocatalytic benzene oxidation by $H_2O_2$ under visible light. In 2013, Zhang *et al.* reported the $FeCl_3^-$ mesoporous $C_3N_4$ combined material ($FeCl_3$/mpg-$C_3N_4$) as a photocatalyst to activate $H_2O_2$ for the oxidation of benzene to phenol under visible light.[56] The fast reduction of $Fe^{3+}$ to $Fe^{2+}$ by photo-generated electrons from mpg-$C_3N_4$ is crucial to the high activity. More recently, Wang *et al.* reported that ternary hexagonal boron carbon nitride (h-BCN) nanosheets were synthesized by doping biomass glucose *in situ* into hexagonal boron nitride (h-BN).[57] The prepared h-BCN showed high activity for photocatalytic benzene oxidation to phenol in the presence of $H_2O_2$ and $FeCl_3$. The introduction of conductive graphene into this material provides a catalyst that combines the advantages of graphene and h-BN with good performance in the oxidation of benzene. Fig. 7 shows the photocatalytic reaction conducted in the dual-phase system. The electron from h-BCN under visible light in the organic phase was transferred to the aqueous phase for the reduction of $Fe^{3+}$ to $Fe^{2-}$, which promotes the activation of $H_2O_2$ to produce $^{\bullet}OH$. The $^{\bullet}OH$ radical subsequently attacks benzene to give phenol.

Ye *et al.* reported that ferrocene covalently linked to the $C_3N_4$ exhibited activity for photocatalytic benzene oxidation to phenol with $H_2O_2$.[58] Due to the stable π-conjugation between a molecular iron catalyst and a $C_3N_4$ organo-photocatalyst, the prepared photocatalyst showed high stability, which was confirmed by stability tests and optical characterization.

Metal particle loading effectively increased the activity of $C_3N_4$ for photocatalytic benzene oxidation by $H_2O_2$ under visible light irradiation. Hosseini *et al.* developed an Au–Pd bimetallic-loaded $C_3N_4$ photocatalyst (Au–Pd/$C_3N_4$) using a sol-immobilization approach.[59] In this synthesis method, the Au–Pd nanoparticles were embedded in a $C_3N_4$ matrix, resulting in a very small loading and high nanoparticle distribution. The catalysts combining Au and Pd on $C_3N_4$ showed higher activity than those incorporating only Au or Pd. Density functional theory (DFT) calculations indicated that the simultaneous presence of Au and Pd in the $C_3N_4$ matrix resulted in more probable electron transfers from bimetallic Au–Pd NPs to $C_3N_4$ for $H_2O_2$, leading to a higher phenol yield.

Verma *et al.* investigated some other inexpensive metal particles loaded with $C_3N_4$.[60] They first confirmed that the metal particle without loading on $C_3N_4$ did not show excellent results. Copper (Cu) is an efficient transition metal in $H_2O_2$ activation. The $C_3N_4$-supported Ag–Cu catalysts showed higher activity compared to other dual metal particles. The $^{\bullet}OH$ radicals formed by $H_2O_2$ activation react with C–H bonds of benzene activated on the surface of $C_3N_4$ to form phenol (Fig. 8).

In other research, Pd-combined Cu was loaded on a whole surface of $C_3N_4$.[61] The as-prepared CuPd/$C_3N_4$ composite photocatalysts were tested for benzene oxidation to phenol with $H_2O_2$ under visible light irradiation (Fig. 9a). The uniform distribution of CuPd on $C_3N_4$ improved the light absorption properties of the photocatalyst. The edge of the CB minimum of HCN-5 was up-shifted by 0.39 eV with respect to pristine $C_3N_4$ and HCN. This up-shift of the CB promoted the reduction of electrons in the CB, enhancing the photocatalytic performance of benzene oxidation to phenol. From the result of the reaction mechanism, $^{\bullet}OH$ and $O_2^{\bullet-}$ were the main reactive species for benzene oxidation. Due to the electron trap ability of CuPd, the photogenerated electron from $C_3N_4$ reacted with $O_2$ to $O_2^{\bullet-}$ and $^{\bullet}OH$. Besides, $H_2O_2$ or $H_2O$ was activated by holes to give $^{\bullet}OH$. The generated $^{\bullet}OH$ radical attacked benzene to produce phenol. In addition, the hole directly oxidized benzene to a benzene cation radical, which reacted with $O_2$ to give phenol in a minor yield. In Fig. 9(b),

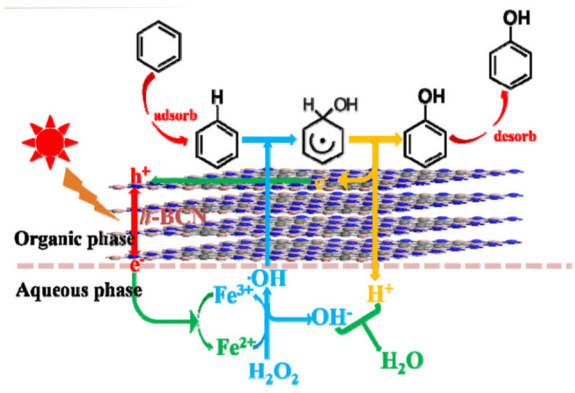


Fig. 7 Reaction mechanism for photocatalytic hydroxylation of benzene by h-BCN combined with $FeCl_3$. Adapted with permission from ref. 56. Copyright 2013 Elsevier.

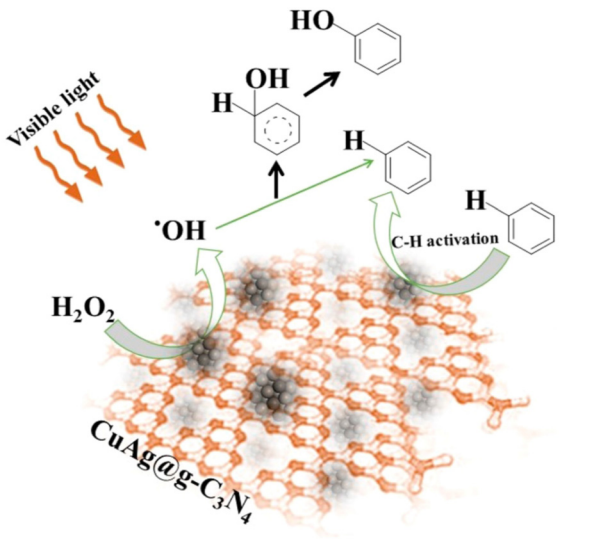


Fig. 8 Plausible mechanism for the hydroxylation of benzene with $H_2O_2$ by CuAg@ $C_3N$. Adapted with permission from ref. 60. Copyright 2017 ACS.

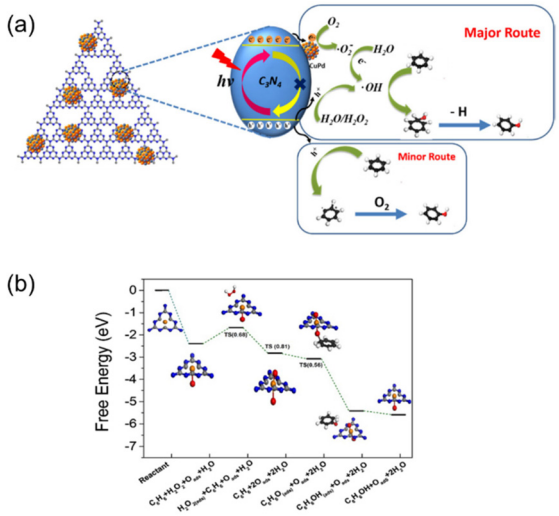


Fig. 9 (a) Plausible mechanism for the hydroxylation of benzene with $H_2O_2$ by CuAg@ $C_3N_4$. (b) Free energies of various structures. Adapted with permission from ref. 58. Copyright 2019 Elsevier.

the calculation result confirms two main steps in the reaction: $H_2O_2$ activation to form $^{\bullet}OH$ and the subsequent selective oxidation of benzene by the generated $^{\bullet}OH$ radical.

More recently, Sun *et al.* synthesized MOF-derived CuO and loaded it on the surface of tubular $C_3N_4$ (CuO/CN) by the high-temperature calcination of the Cu-MOF/TCN precursor (2022).[40] In another work, Cu single atoms were anchored on $C_3N_4$ with the help of abundant N sites to maximize Cu utilization.[62] The above two systems promoted the separation of photogenerated charge carriers due to the incorporation of Cu, resulting in almost full conversion of benzene to phenol using $H_2O_2$ as the oxidant under visible light.

Except for using Cu as a noble metal-free co-catalyst, Devi *et al.* prepared a photocatalyst by modifying $C_3N_4$ nanosheets with a $NiO/WO_3$ nanohybrid *via* a simple ultra-sonication method.[63] This noble metal-free photocatalyst exhibited high activity for photocatalytic benzene oxidation to phenol with $H_2O_2$ under visible light due to heterojunction formation. The electron transfer from $NiO/WO_3$ to $C_3N_4$ facilitated the activation of $H_2O_2$ for $^{\bullet}OH$ and phenol production.

$C_3N_4$ has been well studied for photocatalytic benzene oxidation to phenol due to its tunable activity under visible light. The oxidizing power of $C_3N_4$ is considered relatively mild because $H_2O_2$ is used as the oxidant, and $O_2$ is unavailable.

### 3.3 Metal–organic frameworks (MOFs)

Metal–organic frameworks (MOFs) are hybrid materials with diverse structures used as adsorbents and catalytic materials. MOFs can also be applied to MOF photocatalytic reactions. In 2015, Wang *et al.* developed the first MOF-based photocatalytic system for benzene oxidation with $H_2O_2$.[64] Two kinds of Fe-based MOFs (MIL-100 and MIL-68) have been utilized and compared in this reaction system (Fig. 10). The structure of MOFs significantly influences the photocatalytic performance.

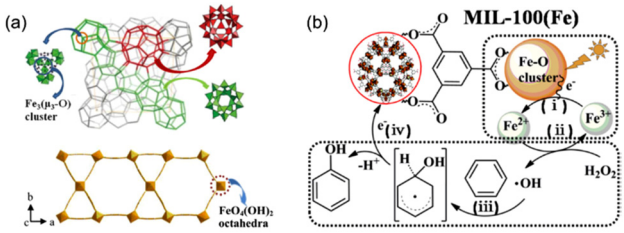


Fig. 10 (a) Topological view of MIL-100 and MIL-68; (b) possible reaction mechanism for the photocatalytic benzene hydroxylation over MIL-100(Fe). Adapted with permission from ref. 64. Copyright 2015 ACS.

The kinetic isotope effect (KIE) study revealed that the reaction obeyed a photo-Fenton reaction mechanism in the presence of Fe. Later, Xu *et al.* synthesized MIL-100 with a uniform size and morphology assisted by glycol. The as-prepared MIL-100 sphere also exhibited high activity for phenol formation.

The variable structure of MOFs plays a key role in the modification of photocatalytic activity. Fang *et al.* prepared a heterogeneous catalyst UiO-66-$NH_2$-SA-V by anchoring vanadium oxy acetylacetonate on the Schiff base UiO-66-$NH_2$-SA (2019).[65] The UiO-66-$NH_2$-SA-V catalyst was used for photocatalytic benzene oxidation using $H_2O_2$ as an oxidant in an acetonitrile and acetic acid mixture. The Zr-MOF material promoted benzene absorption, and $VO(acac)_2$ activated $H_2O_2$ to $^{\bullet}OH$, oxidizing the absorbed benzene to phenol. Thus, the high benzene oxidation performance is attributed to the synergetic effect between the Zr–MOF and the vanadium complex. More recently, Xu *et al.* incorporated the Keggin-type vanadium-substituted polyoxometalate ($PMo_{10}V_2$) into the MOF ($NH_2$-MIL-88/$PMo_{10}V_2$) material with strong interaction between positively charged $-NH^{3+}$ of the support and the negatively charged Keggin anion (2021).[66] The as-prepared composites showed high activity for photocatalytic benzene oxidation to phenol with $H_2O_2$. Both $PMo_{10}V_2$ and Fe promoted the activation of $H_2O_2$ to produce $^{\bullet}OH$ for the subsequent benzene oxidation reaction. Furthermore, the recycling experiments and FTIR analysis proved the high stability of $NH_2$-MIL-88/$PMo_{10}V_2$. Wang *et al.* decorated MIL-53-$NH_2$ with Fe and Cr single atoms.[67] The Fe and Cr atoms act as electron donors and electron acceptors respectively, which promoted charge separation during the photocatalytic process. As a result, an enhanced photocatalytic benzene oxidation to phenol has been achieved in this system.

### 3.4 Tungsten oxide ($WO_3$)

Tungsten oxide ($WO_3$) is another type of semiconductor-based photocatalyst that attracted wide attention recently due to its advantages, such as nontoxicity, physicochemical stability, and low cost.[68–70] As an Earth-abundant metal oxide, $WO_3$ is an n-type semiconductor with a band gap between 2.4 and 2.8 eV and is active under visible light.[71] Pristine $WO_3$ usually showed poor activity because of the fast recombination of light-induced electrons and holes. Appropriate co-catalysts

(especially noble metals such as Pt, Pd, and Au) are commonly needed and enhance the photocatalytic activities of $WO_3$.[72]

Tomita *et al.* modified commercially available $WO_3$ with Pt nanoparticles to obtain $Pt/WO_3$, which can synthesize phenol by photocatalytic oxidation of benzene with $O_2$ under UV irradiation (2014).[73] Compared to $Pt/TiO_2$, $Pt/WO_3$ exhibited a much higher yield and selectivity of phenol due to a different photocatalytic reaction mechanism. In benzene oxidation on $TiO_2$, the main route was the direct oxidation of adsorbed benzene to form a benzene cation radical, which was subsequently converted to phenol. On the other hand, the adsorption capacity of $WO_3$ for benzene was relatively low, and benzene oxidation proceeded through an indirect pathway where $WO_3$ first oxidizes $H_2O$ to the $^{\bullet}OH$ radical, which activated benzene to form phenol.

Kurikawa *et al.* investigated Pt nanoparticle-loaded commercial $WO_3$ ($Pt/WO_3$) for photocatalytic benzene oxidation to phenol with $O_2$.[74,75] They reported that the phenol yields under visible light irradiation were much lower than those obtained under UV irradiation. Furthermore, the reaction mechanism under visible light was different from that under UV light irradiation. In this system, the reduction of $O_2$ to $H_2O_2$ at the Pt surface was critical to phenol formation. Besides, Ohno *et al.* developed stabilized subnanometer $WO_3$ quantum dots for an efficient noble metal-free photocatalyst for benzene oxidation with $O_2$ under UV light irradiation.[76] The quantum size effect successfully controlled the band structure of the $WO_3$ photocatalyst. As shown in Fig. 11, an increase in the band gap of $WO_3$ and an upshift of CB occurred, which increased the rate for the photocatalytic oxidation of benzene to phenol. These studies revealed that $WO_3$ is an efficient photocatalyst for benzene oxidation with $O_2$ under aerobic conditions other than $TiO_2$ because the phenol selectivity is higher with $WO_3$. In addition, noble metal particles are commonly needed as cocatalysts to increase the activity for photocatalytic benzene oxidation in the $WO_3$ systems.

Recently, our group reported that a Pt-loaded 1D monoclinic $WO_3$ nanorod (Pt/m-WNR) shows higher activity than other $WO_3$ structures, due to the significant effect of the crystal phase and morphology (Fig. 12a).[77] In this work, an oxygen reduction mechanism has been proposed for benzene oxidation to phenol over Pt/m-WNR based on both experimental and DFT calculation results (Fig. 12b and c). This oxygen reduction mechanism is significantly distinct from the water oxidation mechanism or direct hole oxidation mechanism in the other reported photocatalytic systems. Based on the oxygen reduction mechanism, the crucial role of the work function and Schottky barrier on oxygen reduction over different $WO_3$ crystal structures has been further proposed by DFT calculations.

### 3.4 Other heterogeneous photocatalysts

Semiconductor-based materials are the major heterogeneous photocatalysts for benzene oxidation to phenol with $H_2O_2$ and $O_2$. Some other heterogeneous photocatalysts have recently been reported for benzene oxidation to phenol. Zhang *et al.* prepared polyoxometalates paired ionic salts (IL-POMs) using quinoline cations with Keggin-type phosphotungstic (PW) anions (2019).[78] The complex contains two photocatalytic ions, an organic molecule, quinolinium salt, and an inorganic molecule, POM, whose photocatalytic properties can be modulated by changing the anions of the organic cation and POM.

Gu *et al.* prepared a series of supramolecular catalysts based on alkoxohexavanadate anions and quinolinium ions for photocatalytic benzene hydroxylation.[79] They clarified the crucial role of the synergistic effect of quinolinium salt and POMs, in which the *in situ* $H_2O_2$ generation was important for benzene oxidation, as shown in Fig. 13. The length of the carbon chains could easily modify the pore structure of photo-

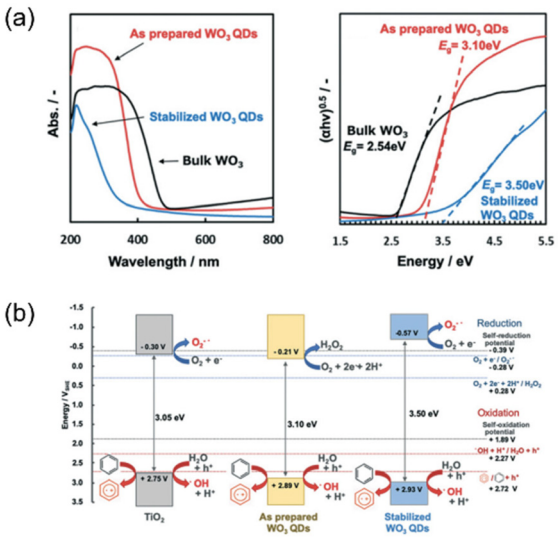


**Fig. 11** (a) Uv-vis spectra of different $WO_3$ structures; (b) Proposed reaction mechanisms for phenol production over $Pt/WO_3$ and $Pt/TiO_2$ photocatalysts. Adapted with permission from ref. 76. Copyright 2021 RSC.

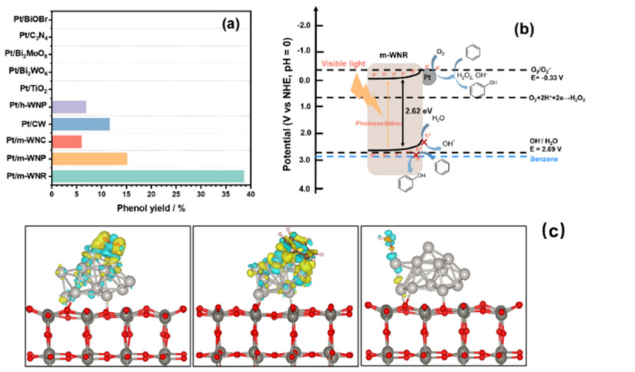


**Fig. 12** (a) Photocatalytic benzene oxidation to phenol over different photocatalysts under visible light. (b) Proposed mechanism for photocatalytic benzene oxidation to phenol over Pt/m-WNR. (c) Charge density differences of $O_2$, benzene, and $H_2O$ adsorption on Pt13/$WO_3$(002), respectively.

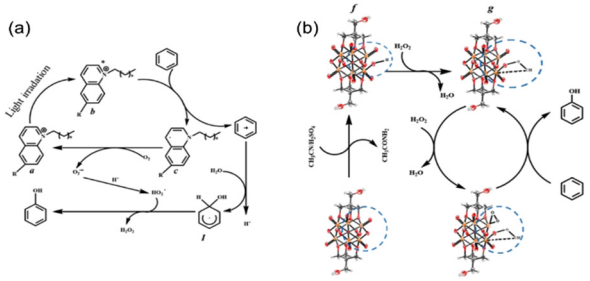


**Fig. 13** The proposed mechanism of hydroxylation of benzene by supramolecular catalysts, $O_2$, $H_2O/CH_3CN$ and $H_2SO_4$ under light irradiation conditions. Adapted with permission from ref. 79. Copyright 2021 Wiley.

catalysts. The longer the carbon chains of quinolinium ions, the larger the pores and channels formed in supramolecular catalysts, and the higher the catalytic efficiency and high phenol selectivity obtained. The comprehensive mechanism study revealed that the reaction includes two steps. First, phenol and $H_2O_2$ are produced by quinolinium ions under photocatalytic conditions. Second, it produced $H_2O_2$, which was then exploited further by the catalytic activation of the alkoxohexavanadate anion to oxidize benzene again.

The photocatalytic hydroxylation of benzene to phenol can be achieved by using several types of catalysts such as $TiO_2$, $C_3N_4$, $WO_3$, MOFs, and others. Their performances are summarized in Table 2. Except for $TiO_2$, most of them can be activated by visible light irradiation using $H_2O_2$ as the oxidant. The $WO_3$ based photocatalyst can actively oxidize benzene under visible light by $O_2$. The unique performance of $WO_3$ can be attributed to the suitable band structure which promotes the $O_2$ activation under mild conditions.

## 4. Strategies for increasing phenol selectivity

Photocatalysts have the advantage of being able to activate benzene molecules under mild conditions. However, as described above, photocatalytic phenol synthesis generally has low phenol selectivity because of the tendency for overoxidation of phenol products. The proposed process for photocatalytic benzene oxidation is shown in Fig. 14. Benzene can also be directly oxidized to $CO_2$ when the photocatalysts have a strong oxidation ability.

Several strategies have been employed to improve the selectivity of phenol in photocatalytic benzene oxidation, which can be broadly classified into the modification of photocatalysts and the change of external operational conditions (Fig. 15). Photocatalysts can be utilized for benzene oxidation reactions because light irradiation activates the photocatalyst, producing active species and free radicals ($^{\bullet}OH$, $O_2^{\bullet-}$, and $HO_2^{\bullet}$). Modification of the photocatalyst by establishing composite structures of photocatalysts, such as metal loading, heterojunction formation, or modification of bandgaps, adjust the generation behavior of these active species and free radicals, which can increase phenol selectivity. Besides, the adsorption properties of benzene and phenol on the catalyst surface are recognized as an important factor in phenol selecti-

**Table 2** Catalytic performance of heterogeneous photocatalysts for benzene oxidation to phenol

| Photocatalysts | Reaction conditions | Yield/% | Sel./% | Ref. |
|---|---|---|---|---|
| $TiO_2$ | 450 W xenon lamp ($\lambda$ > 300 nm), 20 mM benzene, $O_2$, aqueous acetonitrile solution (4 vol%), 4 h | 3 | 86 | 37 |
| $Ti_{1-x-y}M_{x+y}O_2$ | 450 W mercury lamp ($\lambda$ = 200–400 nm), 1 mL benzene, $H_2O_2$, 2 mL acetonitrile, 12 h | 25 | 90 | 43 |
| $Pd/CeO_2/TiO_2$ | 20 W domestic cool LED, 200 mM benzene, $H_2O_2$, 5 mL acetonitrile, 0.5 h | 96 | 99 | 45 |
| $Ti_{0.98}V_{0.02}O_2$ | 400 W mercury lamp ($\lambda$ = 200–400 nm), 1 mL benzene, $H_2O_2$, 2 mL acetonitrile, 24 h | 11 | 85 | 47 |
| $Cu/TiO_2$/CNT | Low pressure mercury lamp ($\lambda$ = 200–400 nm), 20 mM benzene, $O_2$, acetonitrile, 5 h | 52 | 76 | 48 |
| Fe-g-$C_3N_4$/SBA-15 | 500 W mercury lamp ($\lambda$ > 420 nm), 0.8 mL benzene, $H_2O_2$, 4 mL acetonitrile, 4 h | 12 | — | 54 |
| Fe-CN/TS-1 | 300 W xenon lamp ($\lambda$ > 420 nm), 0.8 mL benzene, $H_2O_2$, 4 mL acetonitrile, 4 h | 10 | 18 | 55 |
| $FeCl_3$/mpg-$C_3N_4$ | 100 W mercury lamp ($\lambda$ > 420 nm), 4.5 mmol benzene, $H_2O_2$, 4.5 mL acetonitrile, 4 h | 37 | 97 | 56 |
| h-BCN, $FeCl_3$ | 300 W mercury lamp ($\lambda$ > 420 nm), 0.8 mL benzene, $H_2O_2$, 4 mL acetonitrile, 4 h | 14 | 88 | 57 |
| Fc-MCN | 300 W xenon lamp ($\lambda$ > 420 nm), 0.8 mL benzene, $H_2O_2$, 4 mL acetonitrile, 4 h | 10 | 19 | 58 |
| Au–Pd@g-$C_3N_4$ | 100 W mercury lamp ($\lambda$ > 420 nm), 1 mL benzene, $H_2O_2$, 5 mL acetonitrile, 2 h | 26 | 100 | 59 |
| CuAg@g-$C_3N_4$ | 100 W mercury lamp ($\lambda$ > 420 nm), 1 mmol benzene, $H_2O_2$, 5 mL ethanol, 0.5 h | 99 | 99 | 60 |
| $CuPd/C_3N_4$ | Solar simulator (Sun 2000, ABET), 0.5 mL benzene, $H_2O_2$, 60 mL mixture of acetonitrile and $H_2O$ (v/v = 1 : 1), 1.5 h | 88 | 90 | 61 |
| CuO/CN | 1 mmol benzene, $H_2O_2$, 6 mL acetonitrile, 12 h | 99 | 99 | 40 |
| $NiO/WO_3$@g-$C_3N_4$ | LED light, 2 mL benzene, $H_2O_2$, 10 mL acetonitrile, 50min | 84 | 99 | 63 |
| MIL100(Fe) | 300 W xenon lamp ($\lambda$ > 420 nm), 0.5 mmol benzene, $H_2O_2$, 4 mL mixture of acetonitrile and $H_2O$ (v/v = 1 : 1), 24 h | 23 | 92 | 64 |
| UiO-66-$NH_2$-SA-V | 300 W xenon lamp ($\lambda$ > 420 nm), 1 mL benzene, $H_2O_2$, 6 mL mixture of acetonitrile and acetic acid (v/v = 5 : 1), 4 h | 15 | 100 | 65 |
| $NH_2$-MIL-88/ $PMo_{10}V_2$ | 5 W LED lamp ($\lambda$ = 320–780 nm), 1 mL benzene, $H_2O_2$, 6 mL mixture of acetonitrile and acetic acid (v/v = 1 : 1), 3 h | 12 | 99 | 66 |
| $Pt/WO_3$ | 300 W xenon lamp ($\lambda$ = 300–500 nm), 18.8 μmol benzene, $O_2$, 7.5 mL water, 4 h | 51 | 74 | 73 |
| $Pt/WO_3$ | Blue LED lamp ($\lambda$ = 420–540 nm), 26.8 μL benzene, $O_2$, 10 mL water, 14 h | 14 | 64 | 74 |
| Pt/m-WNR | 300 W xenon lamp ($\lambda$ > 420 nm), 12 μmol benzene, $O_2$, 30 mL water, 1.5 h | 39 | 93 | 77 |
| $C_{16}$Qu-PW | 500 W Mercury lamp ($\lambda \leq$ 365 nm), 1.28 mmol benzene, $O_2$, 1 mL water, 10 h | 21 | 99 | 78 |
| $(C_8\text{-Quin})_2\ V_6$ | UV light, 0.5 mmol benzene, $O_2$, mixture of water and acetonitrile (v/v = 3 : 17), 12 h | 50 | 99 | 79 |

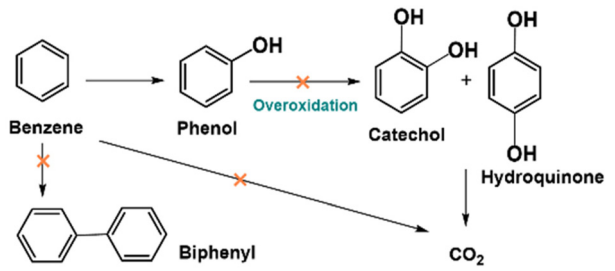


Fig. 14 Photocatalytic oxidation pathways of benzene. The crosses indicate the unwanted reaction pathways.

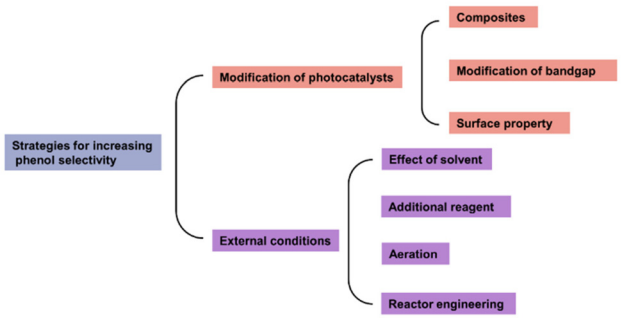


Fig. 15 Strategies for enhancing the photocatalytic selectivity.

vity and can be tuned by modifying the catalyst surface properties. The external operational conditions, including aeration, solvent usage, and utilization of additional reagents, can also control the phenol selectivity in photocatalytic benzene oxidation.

### 4.1 Composite formation

Combining photocatalysts with metal nanoparticles and semiconductors allows efficient control of photocatalytic performance. Marino *et al.* showed that Au nanoparticle loading affects the photocatalytic performance of anatase $TiO_2$ for benzene oxidation (2013).[80] The yield of phenol almost doubled by selecting the appropriate gold loading. This influence of Au decreasing the initial reaction rate but reaching a high phenol yield suggested that gold nanoparticles acted as catalytic sites controlling the reactivity and phenol formation in the photocatalytic process.

Su *et al.* reported a degree of control over the co-catalyst nanoparticle morphology supported on $TiO_2$, which can significantly enhance the product selectivity for photocatalytic benzene oxidation (2014).[81] A systematic series of metal nanoparticles ranging from monometallic Au and Pd to random Au–Pd alloys and core–shell configurations were synthesized by colloidal methods and subsequently supported on a $TiO_2$ (Degussa P25) photocatalyst by a sol-immobilization process. It was found that hydroquinone formation and further polymerization of phenolic compounds could be suppressed using Au as a co-catalyst on $TiO_2$, but the generation of phenol was inhibited. Interestingly, replacing the monometallic Au co-catalyst with Au–Pd core nanoparticles achieved an optimum phenol evolution while hindering hydroquinone formation. The Au–Pd nanoparticles significantly suppressed phenol peroxidation, completely oxidized benzene, and improved the phenol selectivity.

Very recently, Higashimoto *et al.* reported that incorporating metal nanoparticles onto the surface of $WO_3$ also showed enhanced selective phenol formation.[75] This study modified a series of noble metal (Pt, Au, and Pd) and bimetal (Pd/Pt, Pd/Au, and Pt/Au) co-catalysts on the $WO_3$ photocatalysts. The co-catalysts are crucial for $O_2$ reduction for benzene activation during the photocatalytic process. The noble metal co-catalysts and selectivity for photocatalytic benzene oxidation have established a strong relationship. Pt-loaded $WO_3$ showed better performance than $WO_3$ loaded with Au and Pd, which is much higher than that of bare $WO_3$ without co-catalysts. Furthermore, introducing Pt-based bimetal co-catalysts such as Pd/Pt and Pt/Au can further increase phenol formation, due to the enhanced $O_2$ reduction activity.

Semiconductor materials were also utilized to form heterojunctions for the photocatalytic oxidation of benzene to phenol. Chen *et al.* constructed the $Bi_2WO_6/CdWO_4$ hierarchical heterostructure of $Bi_2WO_6$ using $CdWO_4$ micro rods as support materials (2018).[82] The as-prepared $Bi_2WO_6/CdWO_4$ composites showed high phenol selectivity (>99%) in the photocatalytic benzene oxidation with $O_2$. The unique hierarchical heterostructure promoted the separation of photo-induced charge carriers. In addition, the author investigated the crucial role of $^{\bullet}OH$ and proposed a plausible mechanism for the hydroxylation reaction. As shown in Fig. 16, $^{\bullet}OH$ was generated in both water oxidation by photo-generated holes of $Bi_2WO_6$ and $O_2$ reduction by photo-generated electrons. The generated $^{\bullet}OH$ further oxidized benzene as a major reaction pathway. Furthermore, the photoinduced holes efficiently migrated to the CB of $CdWO_4$ and reacted with benzene to form the benzene cation radical as an intermediate which further reacted with $O_2$ to give phenol.

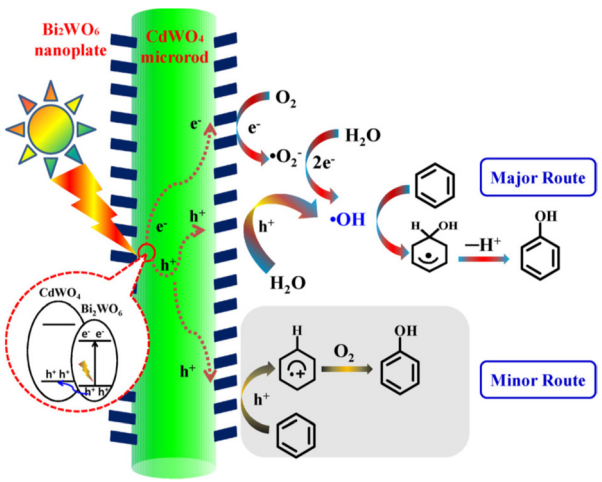


Fig. 16 Plausible mechanism of photocatalytic benzene hydroxylation to phenol over the hierarchical heterostructure of $Bi_2WO_6/CdWO_4$. Adapted with permission from ref. 82. Copyright 2018 Elsevier.

Later, Han *et al.* synthesized Cr-doped CdS/ZnO for photocatalytic benzene oxidation to phenol with $H_2O_2$ under visible light.[83] The result showed that the as-prepared heterostructure exhibited higher phenol selectivity than CdS and ZnO. This enhanced phenol formation is also ascribed to the facilitated separation of photoinduced charge carriers, which improved the electron utilization for $H_2O_2$ activation for benzene oxidation to phenol.

### 4.2 Bandgap modification

The bandgap of semiconductor-based photocatalysts efficiently affects the photocatalytic performance. A suitable conduction band edge can contribute to the generation of superoxide radicals. In a semiconductor with a low position of the CB, photoinduced holes with strong oxidizing properties are formed. This high over potential causes the overoxidation of phenol, resulting in a lower phenol selectivity. For example, ZnO and $TiO_2$, as commonly studied photocatalysts, show high activity for benzene oxidation but low phenol selectivity due to the unsuitable position of the CB. Although chemical doping can modify the band edge position, the existence of the carrier recombination centers produces new sites for the fast recombination of photo-induced charges, thereby restricting their further applications.

Li *et al.* reported a $Zn_2Ti$-layered double hydroxide ($Zn_2Ti$-LDH) photocatalyst with a suitable bandgap (2020).[84] The band position was further modified by the oxygen vacancy in the layer structure of the photocatalysts. As shown in Fig. 17, the top of the VB of $Zn_2Ti$-LDH was 2.52 V *versus* the NHE (pH = 7). Compared to $TiO_2$ and ZnO, the VB edge potential of $Zn_2Ti$-LDH was close to the oxidation potential of benzene (2.48 V). The lower overpotential of $Zn_2Ti$-LDH provides an appropriate thermodynamic driving force for the oxidation of benzene and simultaneously avoids phenol overoxidation. Thus, $Zn_2Ti$-LDH exhibited much higher phenol selectivity than other photocatalysts, including P25, $TiO_2$, and ZnO.

### 4.3 Control of surface properties

Since photocatalytic benzene oxidation always occurs on the catalyst surface under photoirradiation, the selective adsorption ability of the photocatalyst for benzene and phenol is crucial to the phenol selectivity. Thus, it is possible to increase the phenol selectivity by a surface modification to promote phenol desorption from the photocatalysts. For this purpose, specific strategies can be utilized, such as transforming the surface charge/functional group and constructing specific structures.

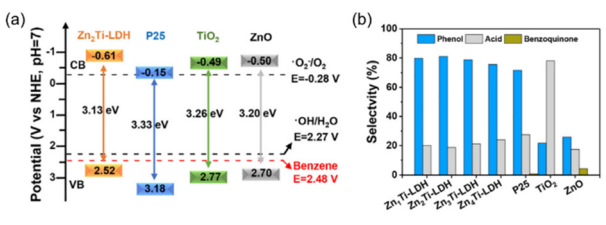


Fig. 17 (a) Schematic band diagrams; (b) selectivity of phenol, acid, and benzoquinone. Adapted with permission from ref. 84. Copyright 2020 Elsevier.

Shiraishi *et al.* developed various mesoporous $TiO_2$ ($mTiO_2$) structures with different pore sizes and surface areas for photocatalytic benzene oxidation to phenol (2005).[85] Based on these photocatalysts, the authors established a photocatalytic activity of $mTiO_2$ driven by an adsorption degree of various substrates, including phenol and phenoxyacetic acid derivatives onto the catalyst surface. This result indicated that phenol was scarcely adsorbed on the surface of $mTiO_2$, and suppressed the subsequent oxidation of phenol. Therefore, $mTiO_2$ exhibited much higher selectivity than $TiO_2$ nanoparticles.

Zhang *et al.* developed a photocatalyst by constructing specific structures and transforming the functional group (2011).[86] $TiO_2$ nanoparticles were entrapped into mesocellular siliceous foam ($TiO_2$@MCF) prepared by the "co-condensation" method. The as-prepared $TiO_2$@MCF was further modified by surface organo-grafting with a silylation agent to make it hydrophobic ($TiO_2$@MCF). Due to the lack of a polar group, benzene was easily absorbed and accumulated in the pore structure of the photocatalyst. After the reaction, the generated phenol was rapidly desorbed due to the hydrophobic properties of the surface, resulting in inhibited phenol oxidation and increased phenol selectivity.

Carbon-based materials are very attractive for catalytic reactions because of their high stability, large surface area, and ability to change surface properties. Recently, some carbon-based materials have been used in photocatalytic benzene oxidation systems to increase phenol selectivity owing to their hydrophobic properties.[87–91] For example, benzene can be selectively oxidized to phenol by reduced graphene oxide (rGO) with $H_2O_2$ under visible light irradiation (2018).[89] The performance for benzene oxidation was significantly improved by more than three times when changing the surface wettability of rGO from hydrophilic (with a contact angle of 52°) to hydrophobic (with a contact angle of 127°). He *et al.* showed that a considerable increase in phenol selectivity could be achieved by modifying the surface of the $Cu_2O$ nanoparticles supported on defective graphene with long-chain alkanethiols (2018).[90] Due to the hydrophobic properties, the modified photocatalysts exhibited much higher phenol selectivity than unmodified samples.

Very recently, Yang *et al.* reported that a carbon shell coated on $ZnFe_2O_4$ significantly enhances the benzene oxidation to phenol with $H_2O_2$, as shown in Fig. 18 (2022).[91] The carbon shell exhibited the composite hydrophobic properties, which promoted benzene accumulation and phenol desorption. As a result, inhibited overoxidation and high phenol selectivity have been achieved. Besides, the carbon shell prevents the leaching of iron species during the reaction, which increases the stability and reusability of the as-prepared photocatalyst.

### 4.4 Solvent optimization

In addition to photocatalytic properties, external conditions affect the selectivity of phenol in benzene photocatalytic oxidation. Our group recently reported that the solvent significantly affects the phenol selectivity in the photocatalytic benzene oxidation by $H_3PW_{12}O_{40}$ using a mixture of water and acetonitrile as the solvent.[21] Phenol oxidation was inhibited by

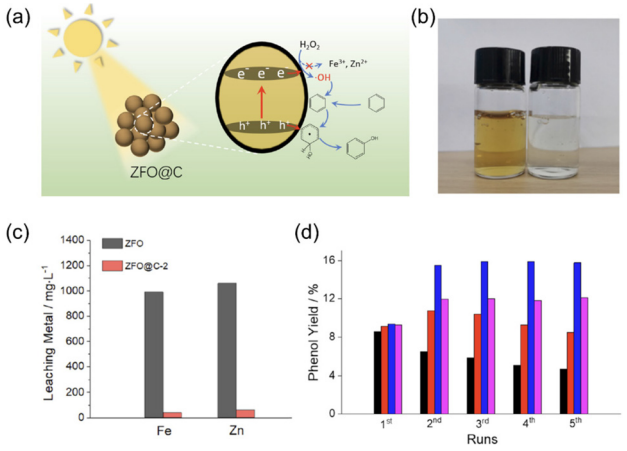


Fig. 18 (a) Photocatalytic hydroxylation of benzene to phenol over ZFO@C; (b) photograph of ZFO (left) and ZFO@C-2 (right) after being acid etched in 1 M HCl for 4 h; (c) ICP results of Fe and Zn leaching from ZFO and ZFO@C-2 during acid etching; (d) photocatalytic synthesis of phenol over ZFO (black), ZFO@C-1 (red), ZFO@C-2 (blue) and ZFO@C-3 (pink). Adapted with permission from ref. 91. Copyright 2022 Elsevier.

adding an optimized amount of acetonitrile as a co-solvent from the experiment result, as shown in Fig. 19a. A large amount of phenol was decomposed in pure water without the addition of acetonitrile. Further investigation revealed that the inhibition of phenol oxidation was due to the suppression of the complexation between phenol and $H_3PW_{12}O_{40}$ by the addition of acetonitrile (Fig. 19b). Thus, the reaction solvent affects the interaction between phenol and the photocatalyst and is an important factor in phenol selectivity.

The solvent can change the reaction process, affecting the phenol selectivity. In another work, we reported that decatungstate is an efficient photocatalyst for benzene oxidation to phenol in acetic acid and water.[39] One-electron and two-electron-reduced decatungstate photocatalysts were observed in benzene oxidation by adding a small amount of acetic acid into a solvent under anaerobic conditions. In contrast, only one-electron-reduced decatungstate has been formed in pure water. The solvent, acetic acid, altered the oxidation reaction process to some extent, favourably promoting the formation of phenol.

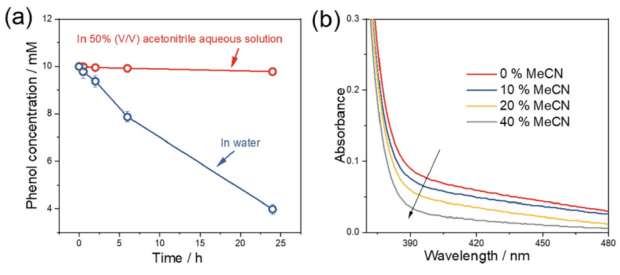


Fig. 19 (a) Time course for phenol decomposition in acetonitrile solution (50 vol%, the red line) and water (the blue line). (b) Changes in the UV-vis absorption spectra of $H_3PW_{12}O_{40}$ in aqueous solution at the acetonitrile concentration.

### 4.5 Additional reagents

The addition of organic compounds such as methanol, ethanol, IPA, and *tert*-butanol to the reaction mixture can alter the active species produced in the photocatalytic system and change the catalytic pathways. In the photocatalytic benzene oxidation reaction, the product phenol is usually utilized as an additional reagent to increase the phenol selectivity. Ide *et al.* first reported that photocatalytic benzene oxidation to phenol in water on Au-nanoparticle-supported layered titanate was accelerated when the reaction was conducted in the presence of phenol (2010).[92] In a more systematic study, Zheng prepared noble-metal loaded $TiO_2$ photocatalysts M@$TiO_2$ (M = Au, Pt, Ag) for benzene oxidation to phenol by adding phenol to the solution (2011).[93] Among the three photocatalysts, the Au@$TiO_2$ catalyst exhibited the highest phenol yield and selectivity. The author proposed that the electron generated on the Au nanoparticle by the surface plasmonic resonance (SPR) effect was transferred to $TiO_2$. Then, this electron was consumed by phenol to generate phenoxy free radicals in the aqueous solution, which was confirmed by the spectroscopic studies. These phenoxy radicals in turn oxidized benzene to phenol, becoming phenoxy anions again. The addition of phenol significantly made the photocatalytic reaction process a more efficient and selective pathway. Furthermore, the author explained the higher activity of Au than those of Pt and Ag in terms of the larger electronegativity of Au which easily oxidized the phenoxy anions to phenoxy radicals.

### 4.6 Reaction atmosphere

$O_2$ is an important oxidant, and in photoreactions in air, $O_2$ dissolves in a solution and participates in the reaction. When $O_2$ in the reaction solution is removed by inert gases such as Ar or $N_2$, the oxidizing ability of the photocatalysts will decrease and subsequently affect the phenol selectivity. Yoshida *et al.* investigated the photocatalytic benzene oxidation in water without $O_2$ to produce phenol and $H_2$ (2008).[94] Phenol was obtained as the main product under these reaction conditions, while benzene degradation mainly occurred with low selectivity to phenol in the presence of $O_2$.

In addition, the presence of $CO_2$ can promote the selective oxidation of benzene to phenol by $TiO_2$-supported Au (Au@$TiO_2$) under light irradiation, as reported by Ide *et al.* (2011).[95] The formation of the successive oxidized products was largely suppressed, and the phenol selectivity significantly increased under a $CO_2$ atmosphere (Fig. 20). On the other hand, various overoxidation byproducts were formed, leading to a low phenol selectivity under an aerobic atmosphere. It is supposed that the $CO_2$ atmosphere suppressed the $CO_2$ generation from successive oxidation of phenol, which increased the yield and selectivity of phenol formation.

### 4.7 Reactor engineering

The reactor design influences the photocatalytic reaction and product separation, which may affect the photocatalytic activity and product selectivity. Molinari *et al.* constructed a photo-

 

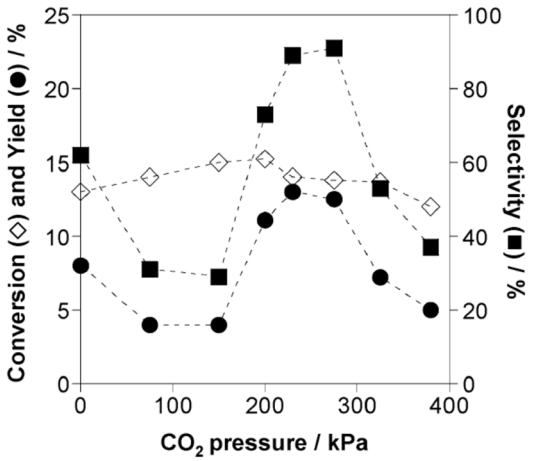


**Fig. 20** $CO_2$ pressure dependence of photocatalytic benzene oxidation to phenol on Au@$TiO_2$. Adapted with permission from ref. 95. Copyright 2011 RSC.

catalytic membrane reactor (PMR) for coupling benzene oxidation and phenol separation together (2009).[96] They showed that using this extractive system suppressed phenol overoxidation. Recently, a continuous-flow microreactor with 2,3-dichloro-5,6-dicyano-*p*-benzoquinone (DDQ) as the oxidant and water as the oxygen source was developed for photooxidation of benzene to phenol under visible light, as shown in Fig. 21 (2021).[97] From the reaction mechanism, the excited state of DDQ (3DDQ*) first oxidizes benzene to form benzene

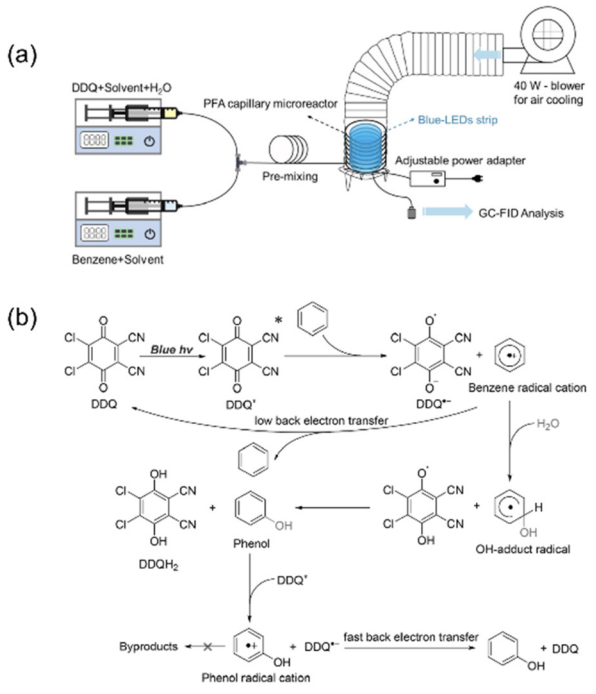


**Fig. 21** System set-up: photocatalytic reactor (a) coupled with the membrane contactor (b); (1: batch reactor, 2: UV lamp, 3: magnetic stirrer, and 4: peristaltic pump). Adapted with permission from ref. 97. Copyright 2021 Elsevier.

radical cations and becomes $DDQ^{\bullet-}$ itself. Then the benzene radical cations react with $H_2O$ to form the hydroxyl radical adducts, which further react with $DDQ^{\bullet-}$ to produce phenol with enhanced efficiency.

## 5. Summary, challenges, and future perspective

One-step photocatalytic benzene oxidation for synthesizing phenol by using $H_2O_2$ and $O_2$ has attracted great attention in the past few decades. The main challenge of this reaction is the high activity of the phenol product, which can be easily overoxidized. Thus, increasing the phenol yield and selectivity is an important research topic. Various homogeneous photocatalysts and heterogeneous photocatalysts have been developed for this reaction. Homogeneous photocatalysts commonly show high activity and phenol selectivity due to good interactions between photocatalysts and benzene molecules. However, they can hardly be recovered after the reaction, which hampers their application. Heterogeneous catalysts, especially semiconductor-based materials including $TiO_2$, $C_3N_4$, and $WO_3$, are the main photocatalysts for benzene oxidation, while their selectivity is generally lower than that of homogeneous photocatalysts.

Several strategies have been developed for increasing the phenol selectivity, including modification of photocatalysts and reaction conditions. An important method for suppressing phenol overoxidation and increasing phenol selectivity is preventing the interaction of phenol and photocatalysts. For example, hydrophobic modification of the photocatalyst surface promotes the fast desorption of phenol to prevent overoxidation. This method can be achieved by using organically modified reagents or directly encapsulating the photocatalyst into a hydrophobic support material that shows low affinity toward phenol. Solvent utilization also affects the interaction between photocatalysts and phenol when using polyoxometalates as catalysts and $O_2$ as an oxidant.

Another method is to reduce the oxidation ability of photocatalysts which is beneficial for the suppression of overoxidation—for example, utilization of semiconductors with low bandgaps and suitable VB band positions. Typical examples of photocatalysts with low bandgaps are $Zn_2Ti$-LDH and $Bi_2WO_6$/$CdWO_4$, which show high selectivity but low activity using $O_2$ as an oxidant. A disadvantage of using these kinds of photocatalysts is the low activity of benzene oxidation due to the high stability of benzene and $O_2$. $C_3N_4$ is another typical visible light photocatalyst with a low bandgap. They have been utilized for photocatalytic benzene oxidation to phenol by using $H_2O_2$ as an active oxidant. Some paper also reported that the atmosphere, namely a $CO_2$ or anaerobic atmosphere, affects the activity and phenol selectivity. The reaction mechanism also affects the phenol selectivity. Phenol can be utilized as a reagent to change the reaction mechanism by introducing a phenol radical to activate benzene molecules and increase phenol selectivity.

Despite the enormous achievements and attempts made in the photocatalytic benzene oxidation to phenol, the enhancement of phenol selectivity is the main challenge, making this research area constrictive. Due to the easy recovery after the reaction, more efforts should be paid to heterogeneous photocatalysts for benzene oxidation. Very few heterogeneous photocatalysts have been reported for benzene oxidation, mainly focusing on $TiO_2$, $C_3N_4$, MOFs, and $WO_3$. Both $O_2$ and $H_2O_2$ have been utilized as oxidants in these photocatalytic systems, where $H_2O_2$ is more easily activated. Photocatalysts with narrow bandgaps and mild oxidation ability, such as $C_3N_4$ and MOFs, only can utilize $H_2O_2$ as an oxidant. However, since $H_2O_2$ is expensive, developing a photocatalytic benzene oxidation system using $O_2$ as the oxidant is desirable. Only $TiO_2$- and $WO_3$-based semiconductor photocatalysts have been reported for benzene oxidation to phenol with $O_2$. Thus, further development of semiconductor-based photocatalysts for benzene oxidation using $O_2$ is required. Attention should be paid to visible light photocatalysts because UV light accounts for only ~5% of solar light. The rational design and synthesis of efficient photocatalytic materials with high phenol selectivity are still challenging. Developing technologies to convert benzene to phenol under mild conditions is required to decentralize chemical industrial processes for decarbonization. The catalytic materials and process designs described in this paper must be refined further.

## Conflicts of interest

There are no conflicts to declare.

## Acknowledgements

This work was supported by the grant from the Science and Technology Research Promotion Program for the Agriculture, Forestry, Fisheries and Food Industry (27006A).

## References

1 C. C. Michelin and N. Hoffmann, *ACS Catal.*, 2018, **8**, 12046–12055.
2 Y. Wu, X. Zhang, F. Wang, Y. Zhai, X. Cui, G. Lv, T. Jiang and J. Hu, *Ind. Eng. Chem. Res.*, 2021, **60**, 8386–8395.
3 L. Zeng, H. Liang, P. An, D. Yu, C. Yang, Y. Hou and J. Zhang, *Appl. Catal., A*, 2022, **633**, 118499.
4 P. Xiao, R. Osuga, Y. Wang, J. N. Kondo and T. Yokoi, *Catal. Sci. Technol.*, 2020, **10**, 6977–6986.
5 L. Meng, X. Zhu and E. J. M. Hensen, *ACS Catal.*, 2017, **7**, 2709–2719.
6 B. S. Rana, B. Singh, R. Kumar, D. Verma, M. K. Bhunia, A. Bhaumik and A. K. Sinha, *J. Mater. Chem.*, 2010, **20**, 8575–8581.
7 M. F. Fellah, I. Onal and R. A. v. Santen, *J. Phys. Chem. C*, 2010, **114**, 12580–12589.
8 O. Shoji, T. Kunimatsu, N. Kawakami and Y. Watanabe, *Angew. Chem., Int. Ed.*, 2013, **52**, 6606–6610.
9 W. Wang, G. Ding, T. Jiang, P. Zhang, T. Wu and B. Han, *Green Chem.*, 2013, **15**, 1150–1154.
10 K. Tian, W.-J. Liu, S. Zhang and H. Jiang, *Green Chem.*, 2016, **18**, 5643–5650.
11 M. Shahami, K. M. Dooley and D. F. Shantz, *J. Catal.*, 2018, **368**, 354–364.
12 J. N. Jocz, Y. Lyu, B. J. Hare and C. Sievers, *Langmuir*, 2022, **38**, 458–471.
13 N. Rahmani, A. Amiri, G. M. Ziarani and A. Badiei, *Mol. Catal.*, 2021, **515**, 111873.
14 A. Mancuso, O. Sacco, D. Sannino, V. Venditto and V. Vaiano, *Catalysts*, 2020, **10**, 1424.
15 A. Mancuso, V. Vaiano, P. Antico, O. Sacco and V. Venditto, *Catal. Today*, 2022, **413–415**, 113914.
16 X. Jia, F. Wang, H. Wen, L. Zhang, S. Jiao, X. Wang, X. Pei and S. Xing, *RSC Adv.*, 2022, **12**, 29433–29439.
17 X. Q. Dua, Y. Ding, F. Y. Song, B. C. Ma, J. W. Zhao and J. Song, *Chem. Commun.*, 2015, **51**, 13925–13928.
18 K. Suzuki, N. Mizuno and K. Yamaguchi, *ACS Catal.*, 2018, **8**, 10809–10825.
19 K. W. Ma, Y. J. Dong, M. Y. Zhang, C. J. Xu and Y. Ding, *J. Colloid Interface Sci.*, 2021, **587**, 613–621.
20 A. Fujishima and K. Honda, *Nature*, 1972, **238**, 37–38.
21 Z. Wang, H. Hojo and H. Einaga, *Chem. Eng. J.*, 2022, **427**, 131369.
22 S. Fukuzumi and K. Ohkubo, *Asian J. Org. Chem.*, 2015, **4**, 836–845.
23 W. Han, W. Xiang, J. Shi and Y. Ji, *Molecules*, 2022, **27**, 5457.
24 K. Ohkubo, T. Kobayashi and S. Fukuzumi, *Angew. Chem., Int. Ed.*, 2011, **50**, 8652–8655.
25 Z. Long, L. Sun, M. Zhang, Y. Zhang, C. Zong, Z. Xue, T. Wang and G. Chen, *Catal. Commun.*, 2019, **121**, 1–4.
26 Y. W. Zheng, B. Chen, P. Ye, K. Feng, W. Wang, Q. Y. Meng, L. Z. Wu and C. H. Tung, *J. Am. Chem. Soc.*, 2016, **138**, 10080–10083.
27 S. Asghari, S. Farahmand, J. S. Razavizadeh and M. Ghiaci, *J. Photochem. Photobiol., A*, 2020, **392**, 112412.
28 J. W. Han, J. Jung, Y. M. Lee, W. Nam and S. Fukuzumi, *Chem. Sci.*, 2017, **8**, 7119–7125.
29 K. Ohkubo, A. Fujimoto and S. Fukuzumi, *J. Am. Chem. Soc.*, 2013, **135**, 5368–5371.
30 A. S. Cherevan, S. P. Nandan, I. Roger, R. Liu, C. Streb and D. Eder, *Adv. Sci.*, 2020, **7**, 1903511.
31 S. S. Wang and G. Y. Yang, *Chem. Rev.*, 2015, **115**, 4893–4962.
32 A. V. Anyushin, A. Kondinski and T. N. Parac-Vogt, *Chem. Soc. Rev.*, 2020, **49**, 382–432.
33 I. A. Weinstock, R. E. Schreiber and R. Neumann, *Chem. Rev.*, 2018, **118**, 2680–2717.
34 C. Streb, K. Kastner and J. Tucher, *Phy. Sci. Rev.*, 2019, **4**, 1–10.
35 N. Li, J. Liu, B. X. Dong and Y. Q. Lan, *Angew. Chem., Int. Ed.*, 2020, **59**, 20779–20793.

 

36 J. J. Walsh, A. M. Bond, R. J. Forster and T. E. Keyes, *Coord. Chem. Rev.*, 2016, **306**, 217–234.
37 H. Park and W. Choi, *Catal. Today*, 2005, **101**, 291–297.
38 M. Schulz, C. Paulik and G. Knör, *J. Mol. Catal. A: Chem.*, 2011, **347**, 60–64.
39 Z. Wang, H. Hojo and H. Einaga, *Mol. Catal.*, 2021, 515.
40 L. Sun, D. Wang, Y. Li, B. Wu, Q. Li, C. Wang, S. Wang and B. Jiang, *Chin. Chem. Lett.*, 2023, **34**, 107490.
41 L. Qin, Z. Feng, Q. Zhang, H. Mao, F. Cheng and S. Shi, *Ind. Eng. Chem. Res.*, 2021, **60**, 13876–13885.
42 S. Farahmand, M. Ghiaci and S. Asghari, *Chem. Eng. Sci.*, 2021, **232**, 116331.
43 P. Devaraji and W.-K. Jo, *Appl. Catal., A*, 2018, **565**, 1–12.
44 S. M. Hosseini, M. Ghiaci, S. A. Kulinich, W. Wunderlich, B. H. Monjezi, Y. Ghorbani, H. S. Ghaziaskar and A. J. Koupaei, *Appl. Surf. Sci.*, 2020, 506.
45 X. Ma, R. Dang, Z. Liu, F. Yang, H. Li, T. Guo and J. Luo, *Chem. Eng. Sci.*, 2020, **211**, 115274.
46 T. D. Bui, A. Kimura, S. Ikeda and M. Matsumura, *J. Am. Chem. Soc.*, 2010, **132**, 8453–8458.
47 P. Devaraji, N. K. Sathu and C. S. Gopinath, *ACS Catal.*, 2014, **4**, 2844–2853.
48 V. D. B. C. Dasireddy and B. Likozar, *J. Taiwan Inst. Chem. Eng.*, 2018, **82**, 331–341.
49 Y. Shiraishi, S. Kanazawa, Y. Sugano, D. Tsukamoto, H. Sakamoto, S. Ichikawa and T. Hirai, *ACS Catal.*, 2014, **4**, 774–780.
50 Y. Yang, Z. Zeng, G. Zeng, D. Huang, R. Xiao, C. Zhang, C. Zhou, W. Xiong, W. Wang, M. Cheng, W. Xue, H. Guo, X. Tang and D. He, *Appl. Catal., B*, 2019, **258**, 117956.
51 X. Zhao, Y. You, S. Huang, Y. Wu, Y. Ma, G. Zhang and Z. Zhang, *Appl. Catal., B*, 2020, **278**, 119251.
52 H. Shi, Y. Li, X. Wang, H. Yu and J. Yu, *Appl. Catal., B*, 2021, **297**, 120414.
53 C. Chu, W. Miao, Q. Li, D. Wang, Y. Liu and S. Mao, *Chem. Eng. J.*, 2022, **428**, 132531.
54 X. Chen, J. Zhang, X. Fu, M. Antonietti and X. Wang, *J. Am. Chem. Soc.*, 2009, **131**, 11658–11659.
55 X. Ye, Y. Cui, X. Qiu and X. Wang, *Appl. Catal., B*, 2014, **152–153**, 383–389.
56 P. Zhang, Y. Gong, H. Li, Z. Chen and Y. Wang, *RSC Adv.*, 2013, **3**, 5121–5126.
57 B. Wang, M. Anpo, J. Lin, C. Yang, Y. Zhang and X. Wang, *Catal. Today*, 2019, **324**, 73–82.
58 X. Ye, Y. Cui and X. Wang, *ChemSusChem*, 2014, **7**, 738–742.
59 S. M. Hosseini, M. Ghiaci, S. A. Kulinich, W. Wunderlich, H. Farrokhpour, M. Saraji and A. Shahvar, *J. Phys. Chem. C*, 2018, **122**, 27477–27485.
60 S. Verma, R. B. N. Baig, M. N. Nadagouda and R. S. Varma, *ACS Sustainable Chem. Eng.*, 2017, **5**, 3637–3640.
61 Y. Zhang and S.-J. Park, *J. Catal.*, 2019, **379**, 154–163.
62 X. Xiao, Y. Gao, L. Zhang, J. Zhang, Q. Zhang, Q. Li, H. Bao, J. Zhou, S. Miao, N. Chen, J. Wang, B. Jiang, C. Tian and H. Fu, *Adv. Mater.*, 2020, **32**, 2003082.
63 M. Devi, B. Das, M. H. Barbhuiya, B. Bhuyan, S. S. Dhar and S. Vadivel, *New J. Chem.*, 2019, **43**, 14616–14624.
64 D. Wang, M. Wang and Z. Li, *ACS Catal.*, 2015, **5**, 6852–6857.
65 Y. Fang, L. Zhang, Q. Zhao, X. Wang and X. Jia, *Catal. Lett.*, 2019, **149**, 2408–2414.
66 P. Xu, L. Zhang, X. Jia, H. Wen, X. Wang, S. Yang and J. Hui, *Catal. Sci. Technol.*, 2021, **11**, 6507–6515.
67 G. Wang, Y. Liu, N. Zhao, H. Chen, W. Wu, Y. Li, X. Liu, A. Li, W. Chen and J. Mao, *Nano Res.*, 2022, **18**, 7034–7041.
68 P. Shandilya, S. Sambyal, R. Sharma, P. Mandyal and B. Fang, *J. Hazard. Mater.*, 2022, **428**, 128218.
69 R. Rajalakshmi, A. Rebekah, C. Viswanathan and N. Ponpandian, *Chem. Eng. J.*, 2022, **428**, 132013.
70 D. Li, Y. Liu, Y. Yang, G. Tang and H. Tang, *J. Colloid Interface Sci.*, 2022, **608**, 2549–2559.
71 S. S. Kalanur, Y.-G. Noh and H. Seo, *Appl. Surf. Sci.*, 2020, **509**, 145253.
72 W. Zhu, J. Liu, S. Yu, Y. Zhou and X. Yan, *J. Hazard. Mater.*, 2016, **318**, 407–416.
73 O. Tomita, B. Ohtani and R. Abe, *Catal. Sci. Technol.*, 2014, **4**, 3850–3860.
74 Y. Kurikawa, M. Togo, M. Murata, Y. Matsuda, Y. Sakata, H. Kobayashi and S. Higashimoto, *Catalysts*, 2020, **10**, 557.
75 S. Higashimoto, Y. Kurikawa, Y. Tanabe, T. Fukushima, A. Harada, M. Murata, Y. Sakata and H. Kobayashi, *Appl. Catal., B*, 2023, **325**, 122289.
76 A. Ohno, H. Watanabe, T. Matsui, S. Somekawa, M. Tomisaki, Y. Einaga, Y. Oaki and H. Imai, *Catal. Sci. Technol.*, 2021, **11**, 6537–6542.
77 Z. Wang, C. Zhu, Z. Ni, H. Hojo and H. Einaga, *ACS Catal.*, 2022, **12**, 14976–14989.
78 L. Zhang, Q. Hou, Y. Zhou and J. Wang, *Mol. Catal.*, 2019, **473**, 110397.
79 Y. Gu, Q. Li, D. Zang, Y. Huang, H. Yu and Y. Wei, *Angew. Chem., Int. Ed.*, 2021, **60**, 13310–13316.
80 T. Marino, R. Molinari and H. García, *Catal. Today*, 2013, **206**, 40–45.
81 R. Su, L. Kesavan, M. M. Jensen, R. Tiruvalam, Q. He, N. Dimitratos, S. Wendt, M. Glasius, C. J. Kiely, G. J. Hutchings and F. Besenbacher, *Chem. Commun.*, 2014, **50**, 12612–12614.
82 P. Chen, L. Chen, Y. Zeng, F. Ding, X. Jiang, N. Liu, C.-T. Au and S.-F. Yin, *Appl. Catal., B*, 2018, **234**, 311–317.
83 W. Han, W. Xiang, Z. Meng, S. Dong and Y. Lv, *Colloids Surf., A*, 2023, **670**, 131529.
84 J. Li, Y. Xu, Z. Ding, A. H. Mahadi, Y. Zhao and Y.-F. Song, *Chem. Eng. J.*, 2020, **388**, 124248.
85 Y. Shiraishi, N. Saito and T. Hirai, *J. Am. Chem. Soc.*, 2005, **127**, 12820–12822.
86 G. Zhang, J. Yi, J. Shim, J. Lee and W. Choi, *Appl. Catal., B*, 2011, **102**, 132–139.
87 D. Wei, L. Huang, H. Liang, J. Zou, W. Chen, C. Yang, Y. Hou, D. Zheng and J. Zhang, *Catal. Sci. Technol.*, 2021, **11**, 5931–5937.

88 Y. Ide, M. Torii and T. Sano, *J. Am. Chem. Soc.*, 2013, **135**, 11784–11786.
89 J. Cai, M. Zhang, D. Wang and Z. Li, *ACS Sustainable Chem. Eng.*, 2018, **6**, 15682–15687.
90 J. He, M. Zhang, A. Primo, H. García and Z. Li, *J. Mater. Chem. A*, 2018, **6**, 19782–19787.
91 B. Yang, S. Zhang, Y. Gao, L. Huang, C. Yang, Y. Hou and J. Zhang, *Appl. Catal., B*, 2022, **304**, 120999.
92 Y. Ide, M. Matsuoka and M. Ogawa, *J. Am. Chem. Soc.*, 2010, **132**, 16762–16764.
93 Z. Zheng, B. Huang, X. Qin, X. Zhang, Y. Dai and M.-H. Whangbo, *J. Mater. Chem.*, 2011, **21**, 9079–9087.
94 H. Yoshida, H. Yuzawa, M. Aoki, K. Otake, H. Itoh and T. Hattori, *Chem. Commun.*, 2008, 4634–4636.
95 Y. Ide, N. Nakamura, H. Hattori, R. Ogino, M. Ogawa, M. Sadakane and T. Sano, *Chem. Commun.*, 2011, **47**, 11531–11533.
96 R. Molinari, A. Caruso and T. Poerio, *Catal. Today*, 2009, **144**, 81–86.
97 X. Shi, S. Liu, C. Duanmu, M. Shang, M. Qiu, C. Shen, Y. Yang and Y. Su, *Chem. Eng. J.*, 2021, **420**, 129976.